

## Supplementary Information on: Chemical insight into electroforming of resistive switching manganite heterostructures

F. Borgatti,<sup>1</sup> C. Park,<sup>2</sup> A. Herpers,<sup>2</sup> F. Offi,<sup>3</sup> R. Egoavil,<sup>4</sup> Y. Yamashita,<sup>5</sup> A. Yang,<sup>5</sup>  
M. Kobata,<sup>5</sup> K. Kobayashi,<sup>5</sup> J. Verbeeck,<sup>4</sup> G. Panaccione,<sup>6</sup> and R. Dittmann<sup>2</sup>

<sup>1</sup>*CNR – Istituto per lo Studio dei Materiali Nanostrutturati (ISMN),  
via P. Gobetti 101, I-40129 Bologna, Italy\**

<sup>2</sup>*Peter Gruenberg Institute (PGI-7) and JARA-FIT*

*Forschungszentrum Juelich GmbH, 52425 Juelich, Germany†*

<sup>3</sup>*CNISM and Dipartimento di Scienze, Università Roma Tre, Rome, Italy*

<sup>4</sup>*EMAT, Electron Microscopy for Materials Science,  
University of Antwerp, Groenenborgerlaan 171, 2020 Antwerp, Belgium*

<sup>5</sup>*NIMS beamline Station at Spring-8,  
National Institute for Materials Science, Sayo, Hyogo 679-5148, Japan*

<sup>6</sup>*CNR – Istituto Officina dei Materiali (IOM),  
Laboratorio TASC, S.S.14, Km 163.5, I-34149 Trieste, Italy*

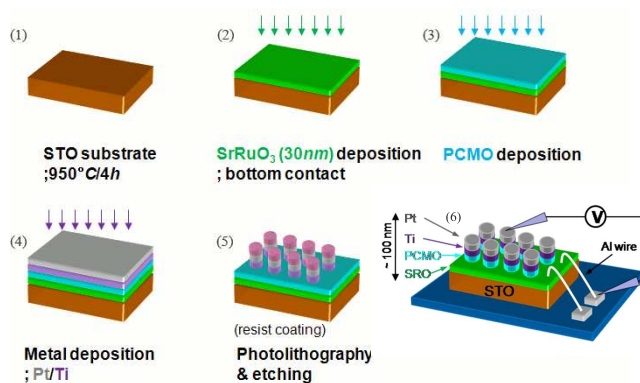


Figure S 1: Sketch of the sample preparation. (1) The STO substrate. (2) SRO and (3) PCMO deposition by PLD. (4) Metal deposition by DC sputtering. (5) TE patterning by photolithography and etching. (6) The completed Ti/PCMO/SRO stack structure.

## I. SAMPLE PREPARATION FOR I-V CHARACTERIZATION

Resistive switching Ti/PCMO/SrRuO<sub>3</sub> (SRO) cells with stack structures with metal-oxide-metal (MOM) configuration have been fabricated. A Pr<sub>0.5</sub>Ca<sub>0.5</sub>MnO<sub>3</sub> (PCMO) thin film was deposited on an epitaxial SRO layer on a single crystal SrTiO<sub>3</sub> (STO) substrate by reflection high energy electron diffraction (RHEED) assisted pulsed laser deposition (PLD). The STO substrate has been TiO<sub>2</sub>-terminated by a treatment with buffered HF and annealing for 2 hours in air at 950 C resulting in a surface roughness of 0.16 nm (RMS). The 30 nm SRO has been grown epitaxially in step-flow growth mode. During the deposition in oxygen atmosphere of 0.133mbar, the substrate temperature was kept at 650 C and the laser energy density was set to 1 J/cm<sup>2</sup>. The PCMO layer was subsequently deposited in a layer-by-layer growth mode using the same oxygen atmosphere, but a fluency 2.8 J/cm<sup>2</sup> and a temperature of 700 C. The layer stack was cooled down in 1 bar oxygen. In the topography of the PCMO thin film, the step-terrace structure of the substrate is reproduced with a roughness of 0.2 nm (RMS). Both films have a X-ray diffraction rocking curves width smaller than 0.045 (FWHM). To complete the MOM structure, a Pt/Ti was deposited on the PCMO/SRO thin film by DC magnetron sputtering and the layered structure was patterned by optical lithography and a dry etching process. An ohmic contact to the SRO layer is provided by using Al wire bonding to a chip carrier with Pt pads.

## II. HOMOGENEOUS VIRGIN AND FORMING STATES

Impedance measurements are very useful tools to separate different resistance contributions by using a Cole-Cole plot with a simulation of an equivalent circuit. Fig. S2(a) shows impedance spectra of virgin states with four different pad sizes. Each impedance spectrum shows two semi-circle combinations which prove that two parallel RC components exist in series. The interface resistance and the bulk resistance were obtained by equivalent circuit simulation. The interface resistance is one order higher than the bulk resistance and both of them clearly show area dependence. Therefore, the resistance of as prepared Ti/PCMO contacts with mixed layers is distributed homogeneously over the entire electrode area. The reliability of the electro-forming process can be demonstrated by using an automatic measurement system with a patterned mask map able to probe more than 100 devices patterned on the same substrate.

Figure S3 shows impedance spectra of the formed states of samples with four different pad sizes. One semi-circle was observed because the bulk resistance is too small compared to the resistance after forming. The resistance after the forming process has increased of about one order of magnitude for all different pad sizes. In Fig. S3(c) the log resistance is in inverse proportion to the log area in which the resistance after forming is nearly homogeneous over the entire electrode area as well.

## III. COMMENTS ON THE IMPEDANCE ANALYSIS

### A. IRS model

In general, the impedance of a metal-semiconductor junction can be modeled as two parallel R-C circuits associated with the Schottky barrier at the interface and a semiconductor-like behaviour in the bulk. However, in our system, the resistance of the PCMO bulk can be ignored in the simulations according to its low resistivity, which we could confirm in our devices by its ohmic contact to Pt and SRO.

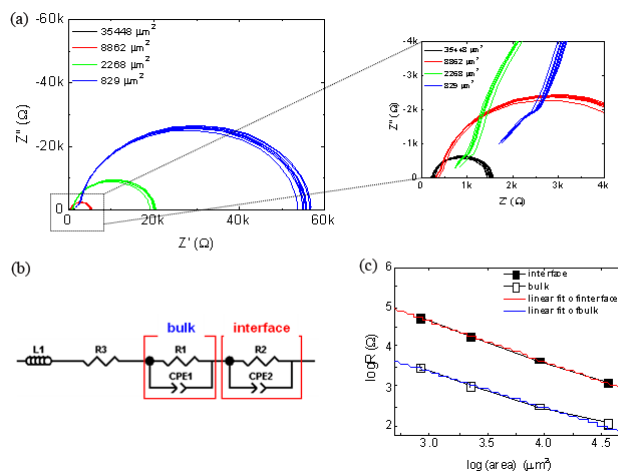


Figure S 2: Homogeneous resistance of virgin states. (a) Cole-cole diagrams of virgin states with four different pad sizes. (b) The equivalent circuit. (c) Area dependence of the interface resistance and the bulk resistance from simulation of the equivalent circuit.

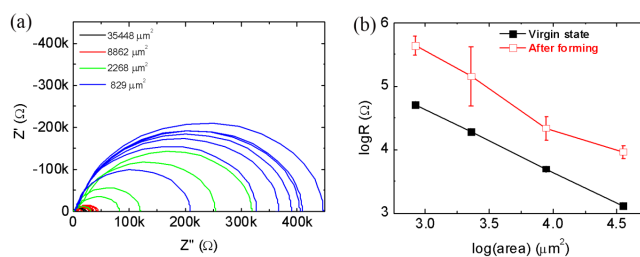


Figure S 3: Homogeneous resistance of forming states. (a) Cole-cole diagrams of forming states with four different pad sizes. (b) Area versus resistance measured at 100 mV of virgin and forming states.

## B. IRS model

The total impedance of the anisotropic  $p$ - $n$  junction should be a series combination of the depletion layer capacitance on the two sides of the junction and the remaining  $n$ -type  $\text{TiO}_x$  layer and the reduced PCMO interface, but we are unable to simulate our data with 4 semicircles. The possible explanation is that (a) the  $\text{TiO}_x$  layer could be considered as a highly doped  $n$ -type conducting semiconductor and could therefore be ignored for the simulations, and (b) if the entire reduced PCMO interface belongs to the  $p$ -type depletion

layer, its contribution would also not be visible in the impedance spectra.

#### IV. SAMPLE PREPARATION FOR TEM/EELS

The TEM samples preparation were performed by Focused Ion Beam (FIB) under exactly the same conditions for devices in the IRS and HRS state fabricated on the same substrate. The devices are indicated by label M8 and M9 for IRS and HRS, respectively. Each slice was chosen horizontally (i.e. parallel to the X direction) as is shown in the figure. No deformation was observed after electroforming.

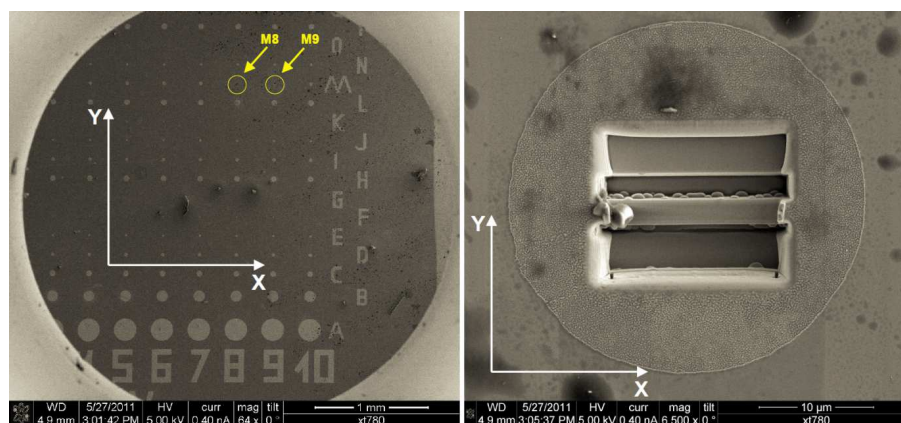


Figure S 4: SEM images of the FIB lamella for TEM measurements.

#### V. SAMPLE PREPARATION FOR HAXPES

Due to the large footprint of the Synchrotron beam, single devices were not suitable for HAXPES measurements and therefore device arrays were fabricated. Fig. S5(a) shows a sketch of the sample layout as seen from above. It consists of a large number of  $100 \times 100 \mu\text{m}^2$  pads with  $10 \mu\text{m}$  spacing between each other, and organized in stripes about 7 mm long and 0.8 mm wide, where every stripe consist of pads in the same resistive state. In this way the X-ray footprint illuminate about 30 pads in the same resistive state. Samples with a thickness of the Ti layer of 10 nm and 7 nm, respectively, were investigated in order to probe different depth regions of the heterostructures. Reference spectra for the SRO were obtained from the part of the sample not covered by the heterostructures, while for the

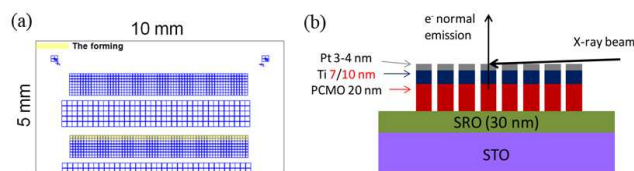


Figure S 5: (a) A schematic layout of the samples and (b) the experimental geometry.

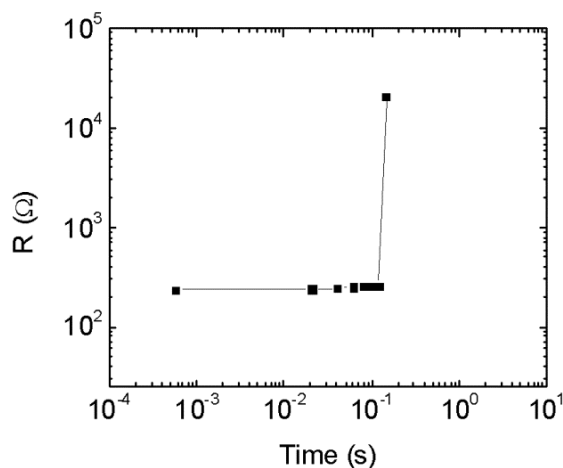


Figure S 6: The threshold DC forming example.

PCMO were acquired from a bare bulk PCMO thick film (50 nm) deposited on STO.

To program the pads for the first forming states an automatic measurement was used with a patterned mask map. A threshold DC forming program was used, in which constant 10 V is applied and the measurement is terminated when the resistance reaches a threshold resistance (5 K ohm), as shown in Fig. S6.

## VI. HAXPES CORE-LEVEL FITTING

The Ti 2p core level spectra have been fitted in the binding energy region 450 – 472 eV. They are partially overlapped to the Ru  $3p_{3/2}$  peak, hence the lineshape of the Ru  $3p_{3/2}$  peak, measured for the bare SrRuO<sub>3</sub>, has been used in the fit analysis. The experimental spectra and the corresponding fit of the Ti 2p spectral region are shown in Fig. S7 where each panel corresponds to the spectrum from a sample with definite Ti layer thickness (7

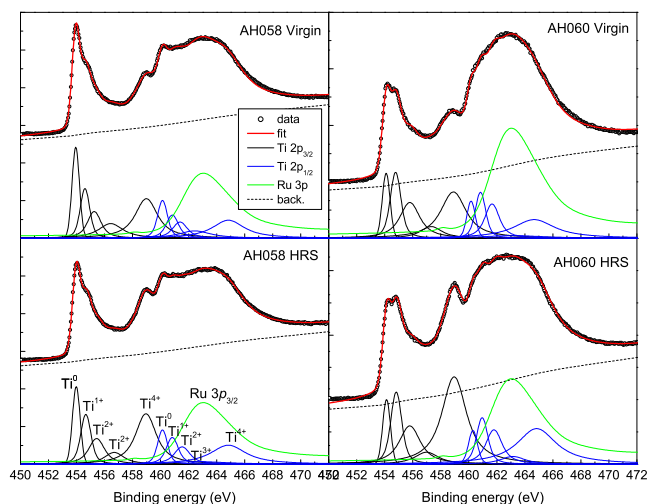


Figure S 7: Fit of the Ti 2p core level spectral region from the samples as indicated in the panels.

or 10 nm) and in a definite resistive state (initial or high resistive state). Open circles are experimental data and red solid line is the best fit to the data, while the dashed line is the integral background. In the fitting curve we have the following components:

- Ru  $3p_{3/2}$  component shown as green line. This curve changes only for a multiplicative factor
- $Ti^0$  : metallic titanium
- $Ti^{1+}$ : non stoichiometric titanium oxide or TiC or TiN. This second supposition is drawn from the binding energy difference between this component and the  $Ti^0$  component, as inferred from Ref. 1
- $Ti^{2+}$ : titanium monoxide (TiO)
- $Ti^{3+}$ : titanium sesquioxide ( $Ti_2O_3$ )
- $Ti^{4+}$ : titanium dioxide ( $TiO_2$ )

Every peak used to fit the Ti 2p levels is a Voigt profile, whose Gaussian part shall represents the experimental energy resolution and the Lorentzian width shall be a measure of the lifetime. The Gaussian full width at half maximum (FWHM) was fixed to be equal for all the peaks and free to vary. Intensity and energy position of the components associated

	Ti 10 nm IRS	Ti 10 nm HRS	Ti 7 nm IRS	Ti 7 nm HRS
	(eV)	(eV)	(eV)	(eV)
Ti <sup>0</sup>	453.95	453.98	454.10	454.13
Ti <sup>1+</sup>	454.67	454.66	454.77	454.82
Ti <sup>2+</sup>	455.66	455.43	455.79	455.79
Ti <sup>3+</sup>	456.75	456.69	457.32	456.99
Ti <sup>4+</sup>	458.95	458.95	458.90	458.96
$\Delta$ Ti <sup>1+</sup>	0.72	0.68	0.67	0.69
$\Delta$ Ti <sup>2+</sup>	1.51	1.45	1.68	1.66
$\Delta$ Ti <sup>3+</sup>	2.79	2.71	3.22	2.86
$\Delta$ Ti <sup>4+</sup>	5.00	4.97	4.80	4.83
<i>S.O.</i>	6.17	6.16	6.06	6.17

Table I: Binding energy position of the peaks associated to the different Ti 2p<sub>3/2</sub> components. The obtained spin-orbit splitting is also indicated (SO) and the energy difference between the different Ti<sup>i</sup> components (i=1+, ..., 4+) and the Ti<sup>0</sup> component is also calculated and indicated as  $\Delta$ Ti<sup>i</sup>.

to the Ti 2p<sub>3/2</sub> level were free parameters, while the energy position of the components associated to the Ti 2p<sub>1/2</sub> level was fixed to literature results<sup>2</sup>, and their intensity fixed to the statistical ratio of 3:2. For what concern the energy position we obtained the results reported in Table I. Note that the results reported are in good agreement with literature results<sup>2,3</sup>.

---

\* Electronic address: francesco.borgatti@cnr.it

† Electronic address: park@IWE.RWTH-Aachen.de

<sup>1</sup> S. V. Didziulis, *Langmuir* **1995**, *11*, 917

<sup>2</sup> J. T. Mayer, U. Diebold, T. E. Madey, and E. Garfunkel, *J. Electron Spectrosc. Relat. Phenom.* **1995**, *73*, 1

<sup>3</sup> E. McCafferty and J.P. Wightman, *Appl. Surf. Sci.* **1999**, *143*, 92